Prediction of Key Crop Growth Parameters in a Commercial Greenhouse Using CFD Simulation and Experimental Verification in a Pilot Study

Subin Mattara Chalill *, Snehaunshu Chowdhury and Ramanujam Karthikeyan

Department of Mechanical Engineering, Birla Institute of Technology and Science Pilani, Dubai Campus, Dubai P.O. Box 345055, United Arab Emirates; snehaunshu@dubai.bits-pilani.ac.in (S.C.); rkarthikeyan@dubai.bits-pilani.ac.in (R.K.)
* Correspondence: p20150006@dubai.bits-pilani.ac.in

Abstract: Controlled crop growth parameters, such as average air velocity, air temperature, and relative humidity (RH), inside the greenhouse are necessary prerequisites for commercial greenhouse operation. Frequent overshoots of such parameters are noticed in the Middle East. Traditional heating ventilation and air-conditioning (HVAC) systems in such greenhouses use axial fans and evaporative cooling pads to control the temperature. Such systems fail to respond to the extreme heat load variations during the day. In this study, we present the design and implementation of a single span, commercial greenhouse using box type evaporative coolers (BTEC) as the backbone of the HVAC system. The HVAC system is run by a fully-automated real time feedback-based climate management system (CMS). A full-scale, steady state computational fluid dynamics (CFD) simulation of the greenhouse is carried out assuming peak summer outdoor conditions. A pilot study is conducted to experimentally monitor the environmental parameters in the greenhouse over a 20-h period. The recorded data confirm that the crop growth parameters lie within their required ranges, indicating a successful design and implementation phase of the commercial greenhouse on a pilot scale.

Keywords: HVAC; CFD; greenhouse; crop growth parameters; box type evaporative coolers (BTEC)

1. Introduction

In regions with harsh climates, it is challenging to provide suitable conditions in terms of temperature, relative humidity, and proper micro-biological environments essential for good crop growth in open farming methods (Ghani et al., 2017) [1]. This is particularly true in the Middle East, as the average temperature during the day is much higher. Scarcity of water makes the conditions even worse. Such adverse conditions preclude open field cultivation, form the backbone of protected agriculture for all weather conditions (Benli 2013) [2], and makes commercial greenhouse farming extremely relevant.

A prerequisite to greenhouse farming is keeping the indoor air velocity, air temperature, and relative humidity (RH) within desired ranges for good crop growth. These three quantities together will be referred to as crop growth parameters in this study. The RH range recommended by agronomists is 45 to 85%, although a tighter RH range of 55 to 65% is sometimes advocated, based on the use of movable dehumidifiers typically employed in commercial greenhouses (Lefers et al., 2016) [3]. The temperature range is more crop-specific; typically, 18–25 °C for most crops, while the desired air velocity range is 0–1.5 m/s. Furthermore, these parameters are interdependent. For example, a small change in temperature will result in a change of RH and the air velocity distribution due to the convection of air.

Establishing a commercially viable greenhouse in the Middle East depends on proper selection of a heating, ventilation, and air conditioning (HVAC) system for cooling the

greenhouse at minimal operational cost. Maintaining a greenhouse temperature between 18–25 °C while allowing for the photosynthetically active region (PAR) of the solar radiation to be transmitted into the greenhouse through the covering material for photosynthesis is a major challenge. Such HVAC systems also have a high energy consumption, leading to high operational costs. Significant efforts are currently been undertaken by greenhouse owners to lower such energy consumption and thereby increase profitability (Taki et al., 2018) [4].

Commercial greenhouses rely on HVAC units along with their controller systems (together called climate management system, (CMS)) to keep the crop growth parameters within the aforementioned specified limits. Such HVAC systems are commonly based on direct evaporative cooling technology, a schematic of such a greenhouse is shown in Figure 1a. In this method, axial fans are mounted at one end of the greenhouse, while honeycomb shaped cooling pads are mounted on the side-walls (far end). Axial fans bring in fresh outdoor air (at a higher temperature than in the greenhouse), which is cooled at the other end by moist, wet cooling pads. Needless to say, the higher surface area of the cooling pads offers enhanced cooling (Dai and Sumathy 2002) [5]. For conventional greenhouses, the number and capacity of the axial fans and the area of the cooling pads are carefully designed and positioned according to HVAC standards (ASHRAE 2011) [6].

(**a**) (**b**)
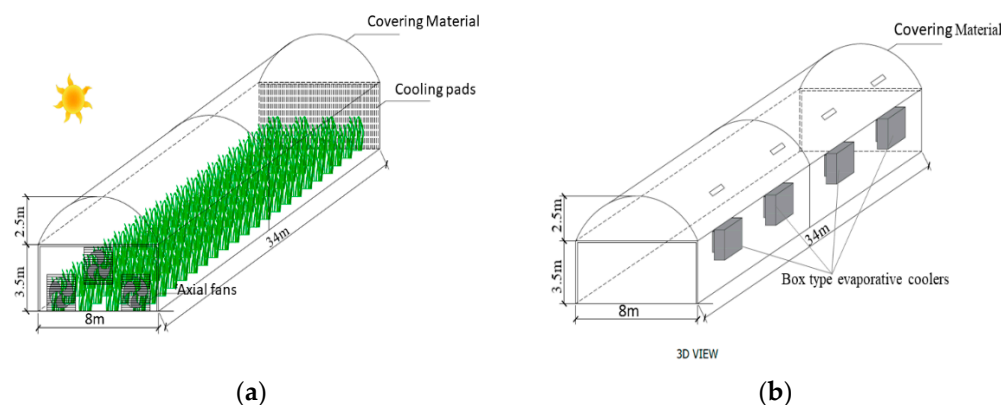
Figure 1. (**a**) Conventional evaporative coolers and (**b**) box type evaporative coolers.

Having axial fans at one end makes it difficult to control the temperature, RH, and air velocity across the entire greenhouse, especially for long greenhouses. Limits on the crop growth parameters have repeatedly been found to be breached in conventional greenhouses, as shown in Figure 1a, causing crop burn and tip burn. This is a consequence of improper design of the HVAC system. These HVAC units, because of the lack of feedback-based climate management systems (CMS), fail to respond to heat load variations, which can change significantly during the course of a hot summer day. The total heat loads due to solar radiation, covering material (Ghasemi Mobtaker et al., 2016) [7], and the ventilation system (Takeshi et al., 2017) [8] must be accurately determined in order to design a suitable HVAC system. In conventional greenhouses, the role of the covering material is not considered. This results in an overdesign of the HVAC system, soaring energy expenditure, and extremely low rate of economic profitability of commercial greenhouses in the Middle East.

Box type evaporative cooling technology is an alternative technology that could be used in greenhouse HVAC systems. A schematic of a box type evaporative cooler (BTEC) is shown in Figure 1b. Instead of being mounted on end walls, such cooling unit(s) are placed along the length of the greenhouse. The number of units required depends on the dimension of the greenhouse. Each individual unit houses a centrifugal fan, allowing for greater control over the air velocity. These units are generally made from high density, temperature resistant poly-ethylene (Perret et al., 2005) [9]. A prior study reported higher mass transfer rates with boxed fans over conventional direct evaporative cooling pad systems (Franco et al., 2014) [10], suggesting a higher energy efficiency. Therefore, it can be

hypothesized that BTEC will be instrumental in reducing operational costs. There is no literature available for the combined effect of BTEC and covering materials in commercial greenhouses for the Middle East climate.

In the recent past, Libin and Xiushui 2011 [11] used CFD simulations to analyze seasonal solar loads and the associated cooling and heating requirements. The determination of the ventilation and cooling requirements of a greenhouse using CFD was carried out by Boulard et al., 2017 and Chu et al., 2017 [12,13]. Considering that BTECs are expensive and their installation is labor intensive, CFD simulations can be quite effective at predicting the distribution of crop growth parameters inside the greenhouse quickly and comparatively inexpensively.

The purpose of this study is therefore twofold. Firstly, a commercial greenhouse is designed to address the shortcomings of conventional HVAC systems by replacing them with BTEC run through an automated CMS. Secondly, we experimentally verify the environmental parameters during a 20-h pilot run in the Emirate of Dubai. The novelty in our design is the use of BTEC coupled to the real-time, feedback-based CMS. To the best of our knowledge, this is the first commercial greenhouse setup in the Middle East using such technology.

2. Methodology

Guided by the objectives of the present study, a two-prong methodology was followed. Initially, a full-scale CFD simulation of the commercial greenhouse using a commercial software, ANSYS Fluent is carried out. The CFD simulation incorporated detailed greenhouse geometry including the BTEC, 2 mm thick polycarbonate as the covering material, and other associated equipment (mentioned later). The capacity of the BTEC was estimated using commercial software named CARRIER® eDesign Software Hourly Analysis Program (HAP), version 5.11. Taking geographical location into consideration, the total heat load calculated was approximately 53 kW. This is equivalent to an air flow rate of 20,999 m^3/h (cubic meters per hour (CMH)). The minimum capacity for side wall mounted BTEC according to the vendor specifications was 25,000 CMH. To keep a factor of safety, we ran our CFD simulation with flow rates of only 50% of this capacity (i.e., 12,500 CMH/cooler). The external air velocity, temperature, and relative humidity were 1.7 m/s, 41 °C, and 52% respectively, at noon on the day of the experiment, and these values are provided as inputs for steady state CFD simulation.

Guided by the CFD results, the necessary BTEC and associated equipment, namely, the HVAC system, were installed. The greenhouse was also fitted with measurement kits and necessary controllers to monitor and record the crop growth parameters (i.e., temperature, relative humidity, and air velocity) at certain locations inside the greenhouse. A climate control module was implemented containing the CMS, which was capable of receiving wirelessly transmitted data from the measurement sensors. A 20-h pilot run was thereafter conducted on a peak summer day.

3. Experimental Setup

3.1. Greenhouse

A standard design model for a greenhouse was suggested by Ghani et al., 2019 [14], for dry environments. The greenhouse must be placed in the east-west (E-W) orientation so as to reduce the amount of solar energy incident on the greenhouse, as this adversely impacts crop growth. The shape of the greenhouse roof should either be in the form of an arc or even shaped, as effective design of the shape minimizes cooling load on the HVAC units.

An experimental single-span greenhouse was built in the Emirate of Dubai in United Arab Emirates for our present study along the suggestions outlined in the ASHRAE handbook. An east-west (E-W) orientation was chosen so as to maximize the daily crop exposure to the sunlight. The exact location in terms of GPS coordinates were latitude: 25°, longitude: 55°, GMT +3.00. A 2 mm thick polycarbonate sheet was used as the covering

material for the roof and the side walls. The floor was covered with moist sand. The roof was in the shape of an arch. This arch type greenhouse was 34.0 m long, 8.0 m wide, 6.0 m ridge height, and 3.5 m eve height. A schematic of the end view of the greenhouse, along with the locations of the various HVAC components, is shown in Figure 2a. Clearly seen are the side wall-mounted BTEC. Figure 2b shows an isometric view of the same greenhouse. Shown in the same figure are the four rows of crops along the length of the greenhouse. The crop height for our present study is 1.7 m. Other relevant details on various material properties pertaining to the greenhouse are given in Table 1.
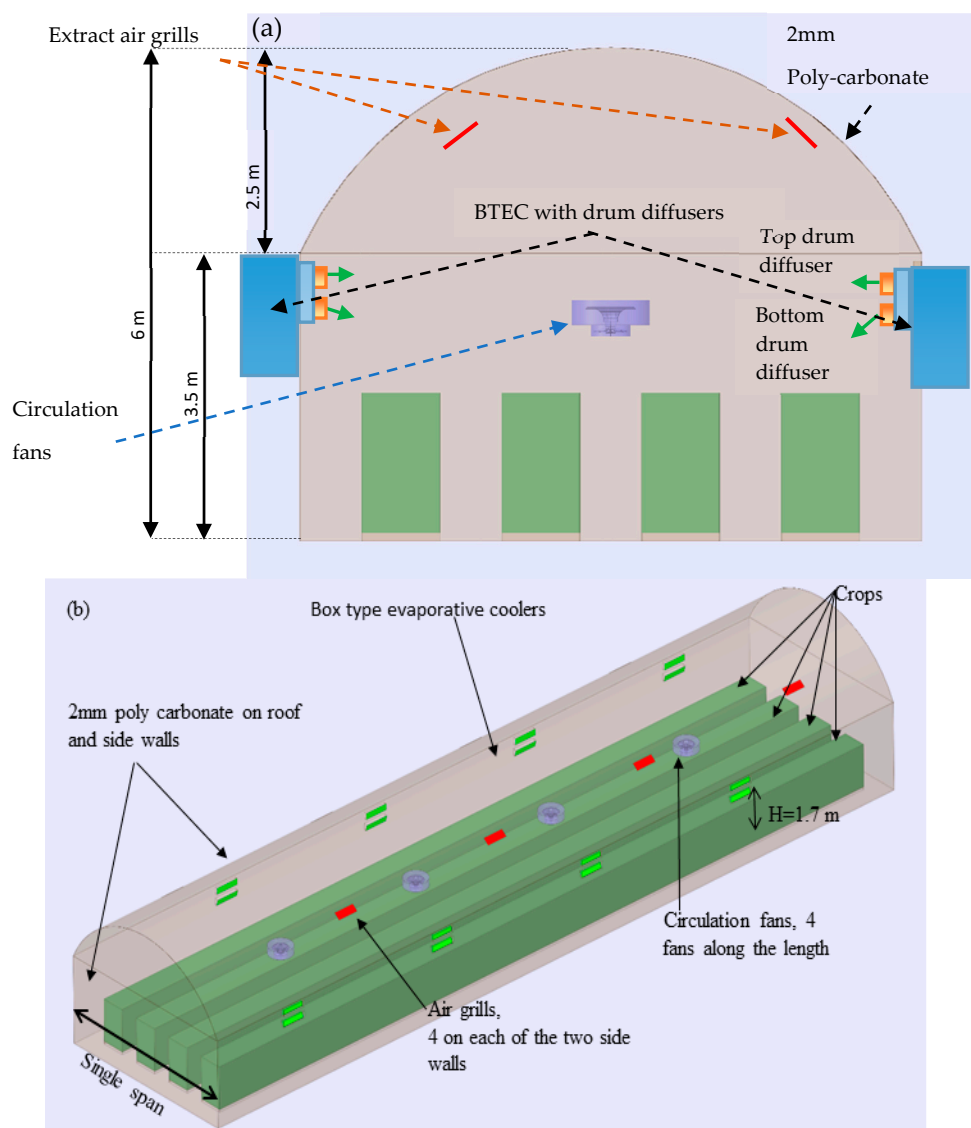
Figure 2. (**a**) 2D front view showing single span greenhouse. Location of the evaporative units, each with two drum diffusers; the extract air grills and the circulation fans are also shown. (**b**) 3D isometric view of the greenhouse. The location of the evaporative units on the side walls along the length of the greenhouse is seen. The heat load locations of the greenhouse used for CFD simulation are also shown.

Major spectral properties such as transmittance, reflectance, and absorbance were recorded based on a spectrometric analysis conducted at the farm. Transmittance is the fraction of the total amount of incident light passing through the covering material and reaching inside the greenhouse, and needs to be accounted for in heat load calculations. Absorbance is the amount of solar light absorbed by the covering material. This will not

pass into the greenhouse, but raises the temperature of the shading material. Reflectance is the amount of light bouncing back from the covering material, and will not pass to the other side and remains unabsorbed. These optical parameters, evaluated by spectrometric analysis of the as received polycarbonate sheets, are used in CFD simulation and are mentioned in Table 1.

Table 1. General properties of the materials used in the greenhouse CFD simulation.

S.No			
1.	**Roof and Side Wall Material**	**Material Property**	**Value**
a		Density (kg m^{-3}) *	1200
b		Thermal conductivity (W m^{-1} $^{\circ}$C^{-1}) *	0.19
c		Specific heat (kJ kg^{-1} $^{\circ}$C^{-1}) *	1.2
d	Polycarbonate sheet	Thickness (mm)	2 mm
e		Transmittance [#]	Total—63.00% Direct—41.00%
f		Reflectance [#]	23.40%
g		Absorptance [#]	14.20%
2.	**Floor**		
		Density (kg m^{-3}) *	1922
	Moist sand	Thermal conductivity (W m^{-1} $^{\circ}$C^{-1}) *	0.25
		Specific heat (kJ kg^{-1} $^{\circ}$C^{-1})	0.8
3.	**Air** [15]		
		Density (kg m^{-3})	1.23
		Thermal conductivity (W m^{-1} $^{\circ}$C^{-1})	0.25
		Specific heat (kJ kg^{-1} $^{\circ}$C^{-1})	0.8

* Obtained from the polycarbonate manufacturer catalogue, [#] Based on in-house spectrometry.

3.2. HVAC System

The HVAC system consists of the BTEC, the air grille (for natural ventilation), and the ceiling mounted circulation fans (for forced ventilation). Almost the entire heat load of the greenhouse is handled by the BTEC and is mostly responsible for bringing in cooler air into the greenhouse. The air grills are mainly responsible for external air flow into/out of the system, depending on the air density gradients. The purpose of the circulation fans is to distribute the air evenly through the greenhouse. Specifications of these components are given in Table 2.

Table 2. Greenhouse HVAC system details.

Equipment (Quantity)	Equipment Parameter	Value (per Unit)
BTEC (8)	Flow rate	25,000 CMH * at full speed
Circulation fans (4, V-flow type)	Rotational speed	1140 rpm
Extract air grills (8)	Size	90 cm $\times$ 30 cm

* Operated at 50% capacity in CFD simulation.

3.2.1. Box Type Evaporative Cooler(s)

A BTEC works with a principle similar to window-mount air conditioners. Each BTEC unit consists of two supply air drum diffusers at the front end (Figure 2a). Cold water flows through a series of tubes behind the diffusers. A centrifugal fan, housed at the rear end of the BTEC, causes a pressure drop as it rotates. The pressure drop is proportional to the revolutions per minute (rpm) of the fan driven by an electrical motor. All of the components come in a sealed box, and as a whole, is called a BTEC. This pressure drop sucks in outdoor hot air. As this air flows over the cold water tubes, it cools down. This cold air is brought into the greenhouse through the two drum diffusers. When mounting on the walls, the diffusers (frontal side) are placed inside the greenhouse while the fan side (rear side) is exposed to the outdoor atmosphere.

Compared with traditional axial fans in conventional greenhouses, centrifugal fans have lower volume flow rates but create a higher pressure difference between the inlet and outlet side. It is this high-pressure gradient that make centrifugal fans more energy efficient than the axial fans, particularly when high volume flow rates are required. BTECs are more durable and easier to maintain.

Each of the drum diffusers can be used to modulate the inlet air flow direction by changing the angle of the axis of the drum diffusers with the horizontal plane. The capacity of each BTEC chosen for our study, from the heat load calculation and vendor specifications, was 25,000 CMH, as mentioned before. As the greenhouse is 34 m long, eight BTECs, four each on the two side walls, were mounted at regular intervals along the length of the greenhouse (see Figure 2a). This was done to ensure uniformity of environmental parameters and eliminate variations along the longest dimension (34 m) of the greenhouse. The upper drum diffuser wa kept entirely horizontal (at 0° angle), while the bottom drum diffusers were angled downward (at 15° downward relative to the horizontal) (refer to Figure 2a). The air velocity, temperature, and RH of the air coming in through these diffusers are mentioned in Table 3. These values are used as input to the CFD simulation.

Table 3. Inlet conditions for drum diffusers and air grills.

Parameter	Value
Supply air drum diffuser	
Inlet velocity	3.18 m/s
Dry bulb air temperature	17 °C
RH for supply air diffuser	97%
Flat supply air grill	
Flow rate from flat supply air grill	0.26 m^3/s
Velocity from flat supply air grill	0.43 m/s
Outside air velocity	1.7 m/s

3.2.2. Circulation Fans

To facilitate the uniformity of crop growth parameters throughout the greenhouse, four horizontal circulation fans were hung from the roof of the greenhouse. This is also mentioned in Table 2. These fans reached a height of 2.5 m from the level of the floor and could be moved along the entire length of the greenhouse using a frame at 2.5 m above floor level (shown in Figure 2b).

3.2.3. Air Grills

Natural convection was maintained using eight symmetrically placed (four on each side) extract and supply air grills located on the arch of the roof along the length (Figure 2b). The specifications of the cooling units used in the greenhouse are given in detail in Table 2.

3.3. Monitoring of Environmental Variables

To monitor the air velocity, temperature, and relative humidity during the pilot run, five measurement kits, labelled 1 through 5, were installed in the greenhouse. This is depicted in Figure 3. Each measurement kit contained a set of two anemometers, a temperature and a relative humidity sensor, and a small data logger (Greystone, CDD5). The anemometers were capable of measuring air velocity between 0 to 1.7 m/s. The response time of the anemometers were on the order of a few seconds. Path length and accuracy of the anemometers were 60 cm and 1.3%, respectively. Each of the five sets (sets 1 through 5) were mounted on a platform that could be varied in height from the floor level ($z = 0$) to a height of $z = 3.5$ m in the vertical direction. In addition, sets 1 through 4 could be moved horizontally along the entire 34 m length of the greenhouse on a pre-determined longitudinal track. Set 5 was placed on a track along the width of the greenhouse and could be moved in a direction transverse to the other anemometer sets. Extreme care was

exercised in the placement and calibration of the anemometers inside each measurement kit so as to minimize measurement errors. Each kit logged its corresponding data in the respective data logger every 20 min. This data were sent to an automated climate control system (CMS) wirelessly, almost instantaneously.
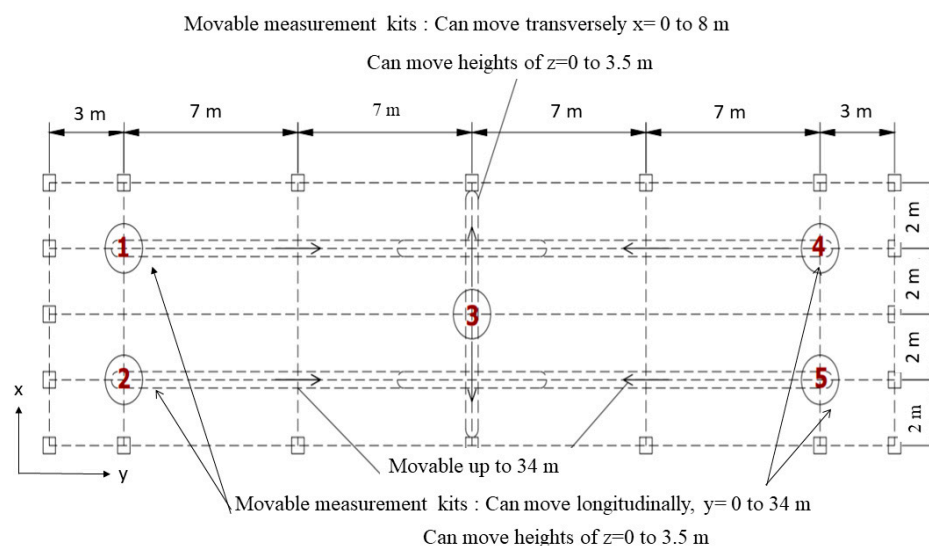
Figure 3. Plan view of instrumentation installed in the greenhouse. Labelled 1 through 5 are individual measurement kits each containing two anemometers, a temperature, a relative humidity sensor, and a small data logger. Kit 3 can move along the width while the other kits move along the length of the greenhouse. All of the kits can be moved up to a height of 3.5 m from the floor level using a movable vertical platform.

External wind speed and direction were measured using a cup anemometer and wind vane, respectively. A potentiometer was used to measure the air-grill vent openings. External ambient conditions were taken from the weather data. All of the measurement kits and HVAC equipment were wirelessly interfaced to an automated climate control system (CMS). All of the data were recorded in the microcomputer of the CMS module every 20 min. The CMS used in this study was a custom built Mamdani model of fuzzy logic-based proportional integral derivative (PID) controllers. The CMS had a central control server, which received data from each of the individual measurement kits as soon as they were recorded. Depending on the measured values of the air velocity, temperature, and relative humidity, the CMS sends a feedback to the individual evaporative coolers, air grills, and the circulation fans. This triggers them to increase/decrease the air flow rates, open/close the air grills, and run the circulation fans faster/slower.

4. CFD Simulation

A full-scale 3D simulation of the greenhouse mentioned above was carried out using ANSYS FLUENT to predict the indoor conditions of the greenhouse over a 20-h period during peak heat load conditions in the summer. This was intentionally chosen, as the cooling load on the HVAC units are maximum during the summer due to the extremely harsh outdoor summer conditions. The 3D polyhedral mesh created had cell sizes varying between 0.5 mm and 200 mm, with a total 6.78 million cells. Good quality mesh was obtained with a maximum skewness of 0.8, minimum orthogonal quality of 0.2, and maximum aspect ratio of 25. A mesh created for the geometry is shown in Figure 4.

(**a**)

(**b**)
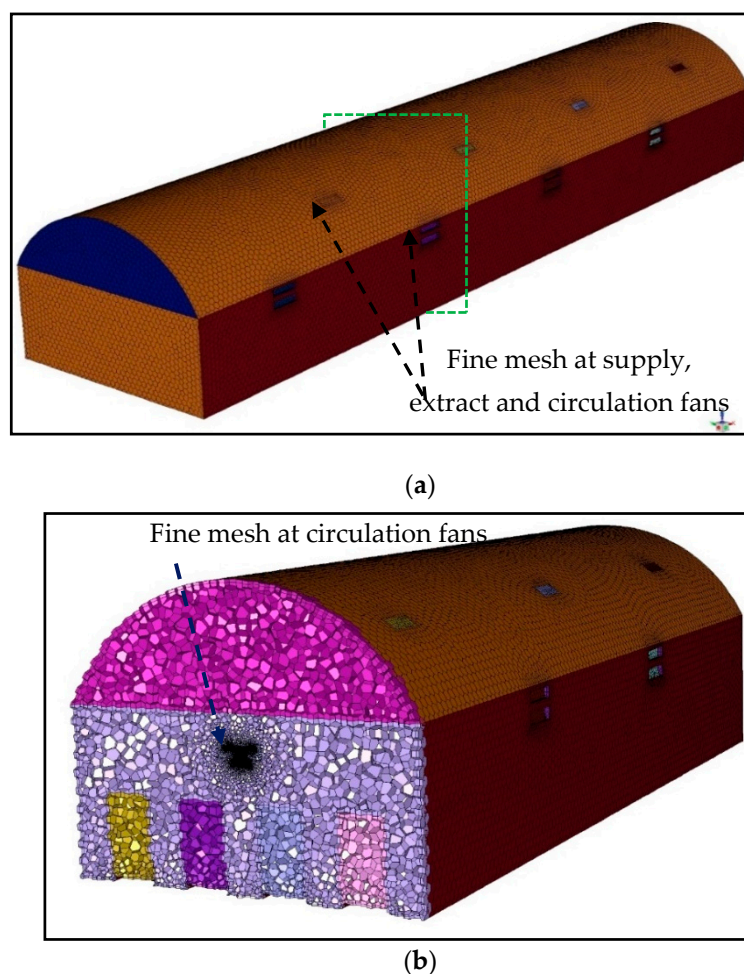
Figure 4. (**a**) 3D isometric view with 0.5 mm mesh and top cut view of the mesh. (**b**) 3D isometric cut view of 0.5 mm mesh of greenhouse.

For an accurate simulation, it was necessary to model the incident solar thermal radiation into the greenhouse for an entire day. For the purpose of our steady state simulation, specific inputs related to the coordinates of the geographical location of the greenhouse, ambient temperature (obtained from weather data), and date were provided to determine the position of the sun and to compute the magnitude of the solar radiation parameters. Heat load entering into the computational domain due to solar radiation through the polycarbonate sheet (roof and side walls) was accounted for by the solar load model available in ANSYS FLUENT. It consisted of a combination of a solar ray tracing algorithm and a radiation model called the surface to surface (S2S) model. The solar ray tracing algorithm worked as the source of the solar heat load and the surface to surface (S2S) radiation model accounted for the internally scattered energy. For the day chosen for our simulation, if the greenhouse was placed at the origin of the coordinate system, then the direction of the sun's rays (i.e., incident solar radiation) was along the line joining the origin of the coordinate system to the point with coordinates are given by $(X, Y, Z) \equiv (-0.143846, -0.0297637, 0.989152)$. The location of the sun was taken at noon. The ambient temperature for our simulation was 41 °C, with an air velocity of 1.7 m/s and 52% relative humidity. Various material properties used for the polycarbonate sheet, floor, and air are already mentioned in Table 1.

The heat gain into the greenhouse was mainly solar radiation through the semi-transparent polycarbonate sheet used for the roof and the side walls, and the heat gain/loss due to other heat transfer modes (conduction and convection) between the greenhouse and the surroundings. These processes mainly involved the natural convection inside the

greenhouse, forced ventilation due to HVAC operation, and conduction in the soil and covering material (Ghani et al., 2019) [14].

The plants were modelled as porous media formulation with 50% porosity. The plant transpiration effect was neglected. The natural extract air grills were assumed to be opened up to 75% of their permissible free area (see Table 1). Additionally, heat gain from one occupant inside the greenhouse was considered with 110 W of sensible heat and 110 W of latent heat. The evaporative coolers were assumed to operate at 50% of their designed capacity (6500 CMH). This is a fair assumption, as the BTECs can run at full capacity if the crop growth parameters (air velocity, temperature, and relative humidity) happen to be outside the desired range of crop growth parameters. For example, if the temperature field obtained in our simulations was outside the desired range, we could run another simulation with the coolers operating at full capacity (or any other fractional capacity) and check whether the temperature lay within the required range. This method could, therefore, serve as a powerful tool to design the installed capacity (flow rate) of the evaporative units and their effectiveness in maintaining controlled conditions inside the greenhouse. Air flow through two alternate circulation fans operating at full capacity was taken into account in the simulation.

Air flow inside the greenhouse was modelled using Reynolds averaged Navier–Stokes equations (RANS). The $k - \epsilon$ turbulence model was used as the flow of air under the conditions encountered in a greenhouse are inherently turbulent due to the low viscosity of air. "k" and "ϵ" refer to turbulent kinetic energy and rate of viscous dissipation, respectively. Further details about this model could be found in Launder and Spalding, 1974 [16]. The air velocity, temperature, and relative humidity were computed by discretizing the computational domain and thereafter solving the continuity Equation (1), the Navier–Stokes Equation (2), and the energy Equation (3) mentioned below.

$$\frac{\partial \rho}{\partial t} + \nabla \rho u = 0 \tag{1}$$

$$\rho \left[\frac{\partial u}{\partial t} + (u \nabla) u \right] = -\nabla p + \nabla \tau + \rho g + f \tag{2}$$

$$\left[\frac{\partial}{\partial t} (\rho E) + \nabla \left(\vec{v} (\rho E + p) \right) \right] = \nabla \left[k_{eff} \nabla T - \sum_j h_j \vec{J}_j + \left(\bar{\bar{\tau}}_{eff} \vec{v} \right) \right] + S_h \tag{3}$$

In these equations, u represents the velocity vector, ρ denotes the density, p denotes pressure, τ the shear stress, g the acceleration due to gravity, f the body force per unit volume, k_{eff} the effective thermal conductivity, T the static temperature, $\vec{J}_j$ the mass diffusion flux of species j, and S_h a source or sink term depending on whether a volumetric heat generation term (source or sink) exists. In Equation (3), $E = h - \frac{p}{\rho} + \frac{v^2}{2}$ and h is sensible enthalpy. Further details regarding their formulation could be found in the ANSYS FLUENT manual [17]. The Equations mentioned in (1)–(3) are solved subject to the boundary conditions. The boundary conditions consider the various distributed heat loads arising due to solar radiation through the covering material, plant load, and electrical appliances inside the greenhouse. The heat loads considered in the CFD simulation are mentioned in Table 4. Relevant inlet boundary conditions for the HVAC system are already tabulated in Table 2.

Table 4. Heat load on the greenhouse used for CFD simulations.

Heat Load Factors	Value (W/m^2)
Solar heat flux through the roof/covering material *	283
Light + circulation fans	281.88

* Obtained using Fluent, based on location and geometry.

A grid independence study was carried out in a manner similar to the procedure developed by Villagran et al., 2019 [18], and the results are shown in Figure 5. The mean values of the crop growth parameters (air velocity, temperature, and relative humidity) were plotted against the corresponding number of mesh elements used for the simulation. The crop growth parameter values were obtained as the area weighted average at a height of z = 1.7 m. This was typically the full-grown height for leafy vegetables selected for this study. A total of four grids with numbers of mesh elements within the range of 0.6 million to 6.75 million were chosen. It is clearly visible from Figure 5 that initially, the crop growth parameters varied with the number of cells, but eventually converged to a stable value as the number of mesh elements in our simulation was approximately 1 million. Therefore, approximately 1,000,000 elements were used for all of the results presented in this article.
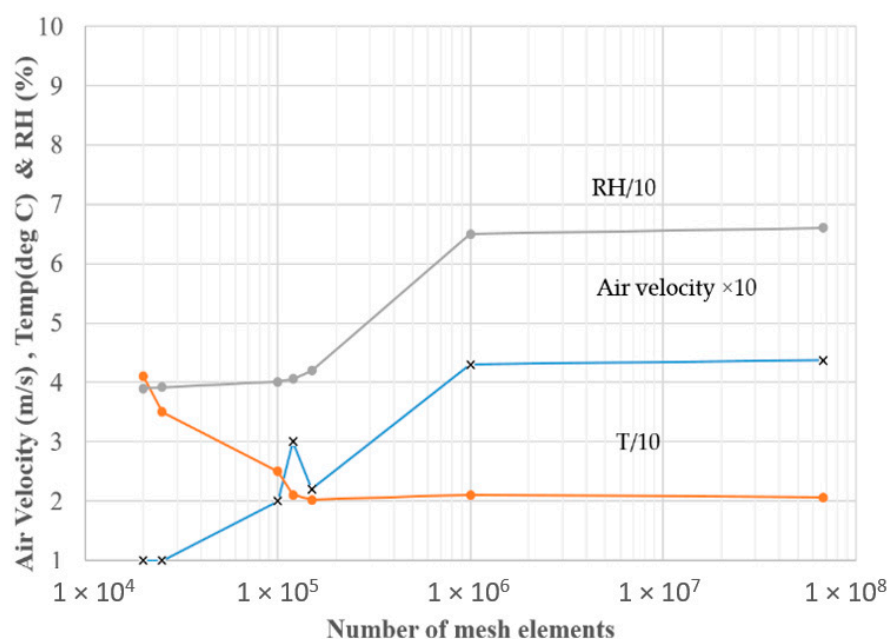
Figure 5. Grid independence study showing the effect of the Air velocity (blue), Temperature (orange) and Relative humidity (gray) as a function of the total number of elements present in the domain. Eventually, a mesh of 10^6 cells were used for faster converged solutions.

5. Simulation Results

The obtained steady-state CFD simulation results for the greenhouse pertaining to the crop growth parameters (i.e., air velocity, temperature, and relative humidity) are first presented in this section. Then, the results of the same parameters recorded experimentally during the pilot-run are mentioned. Finally, a comparison of the predicted and experimental values is made. Before we present the results, it is important to understand some of the limitations/advantages of the both the CFD simulation and experimental data recoded. It is possible to obtain spatially discrete data at almost every location using CFD analysis. Typically, CFD simulations produce cell-averaged data, meaning the parameter value is predicted for a location corresponding to the centroid of the cell. Therefore, by making the cells extremely small (increasing mesh elements), it is theoretically possible to predict the parameter values at every point within the domain. This, however, is extremely expensive in terms of time and computational resources. Therefore, cell weighted averaging was done to obtain the values of any crop parameter at arbitrary locations. These data are presented in the form of contour plots and crop heights shown in Figure 6.
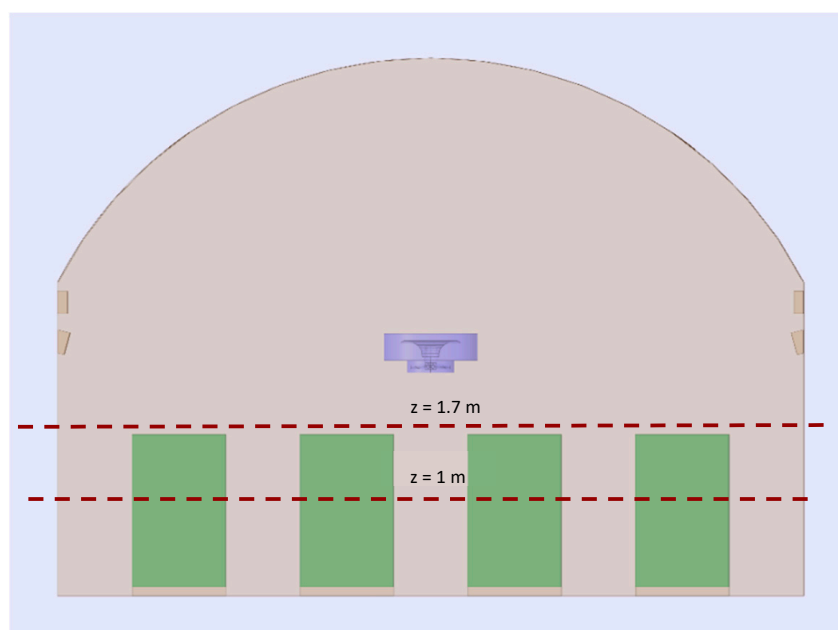
Figure 6. 2D sectional view showing the plane heights.

All of the CFD results presented in this paper are area-weighted averages at certain heights from the floor level of the greenhouse. The heights assume importance because the leafy vegetables used in this study could only grow to a height of 1.7 m. Therefore, we showed the crop growth parameters at two different heights of z = 1.0 m and z = 1.7 m. These two heights will be referred to as occupancy levels 1 and 2 for the greenhouse. Each of the crop growth parameters are discussed in separate subsections below.

5.1. Air Velocity

Various contour plots of air velocity at different planes are shown in Figure 7. It is amply clear from Figure 7a,b, that the air velocity at occupancy level 1 was well maintained within the desired range, as the maximum velocity was about 1.2 m/s. Maximum velocities occur near the side walls at this occupancy level. In Figure 7b, representing occupancy level 2, maximum velocities are about 1.7 m/s. These regions extend from the side wall towards the central region and signify directed air jets. This implies that measurements of air velocity must be taken in those regions and the downward angle on the lower drum diffusers must be reduced from the aforementioned 15° for all of the evaporative coolers during the pilot run. The area-weighted average air velocity at occupancy levels 1 and 2 were calculated to be 0.435 m/s and 0.743 m/s, respectively, which is well within the required specified range.

To investigate the cause of high air velocity in certain regions of the computational domain, a contour plot of the air velocity originating from the evaporative coolers mounted on one of the side walls is shown in Figure 7c. The velocity at the entry from the drum diffusers is observed to be higher than the specified range. A high velocity is also noticed at the air grills, which provide natural ventilation. This is further corroborated in the vector plot of the air velocity at the evaporative coolers located on the same side wall. Therefore, forced ventilation in the form of circulation fans must be used during the trial run. Plant leaves normally show resistance to the air velocity, and that is the reason the air velocity was less for occupancy level 1 compared with occupancy level 2.

Moureh et al., 2002 [19], recorded similar air velocity trends in their studies in a reefer container. Previous studies have resulted in area weighted average velocity in the range of 0.2–0.46 m/s between heights of 1–1.7 m above floor level in 2006 [20,21]. In all the previous studies [19,21], higher ambient air velocity outside the greenhouse resulted in increased air velocity inside the greenhouse. The covering material often shakes at certain air velocities

and this can stir up the inside air, contributing to higher indoor air velocities [20]. This issue has been minimized by using a thick and materially strong covering material (2 mm polycarbonate sheet) instead of conventional polyethylene covering materials.

(**a**)

(**b**)

Figure 7. *Cont*.

(c)
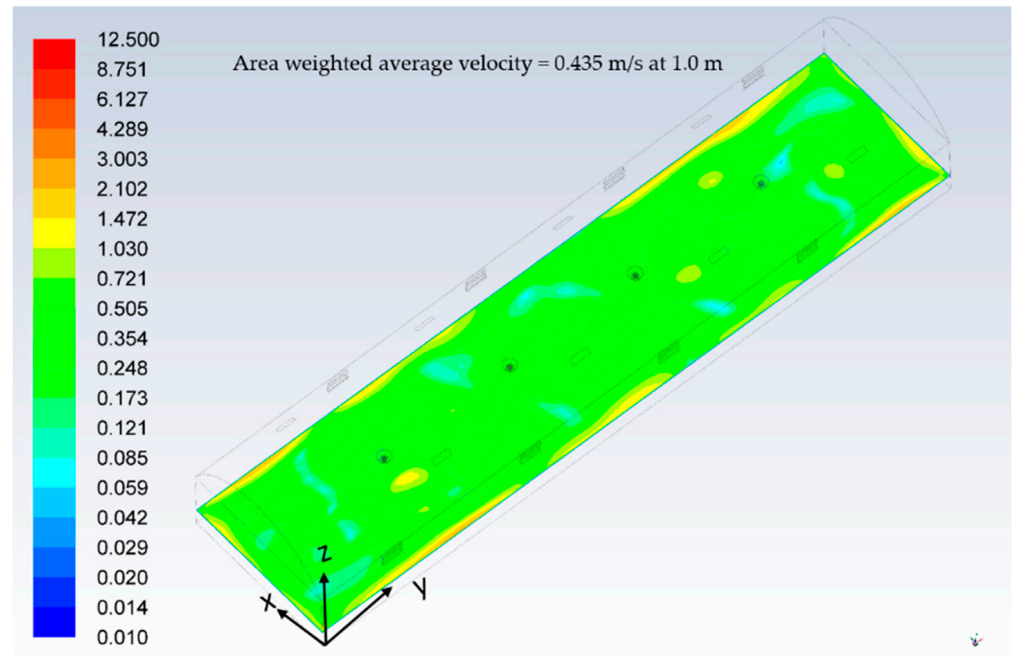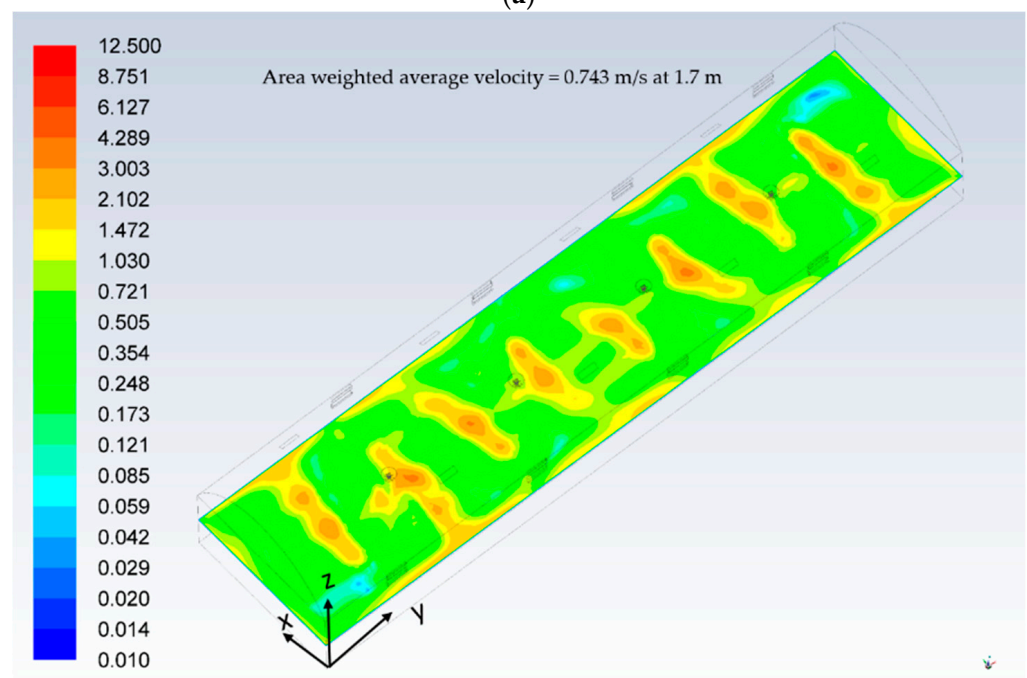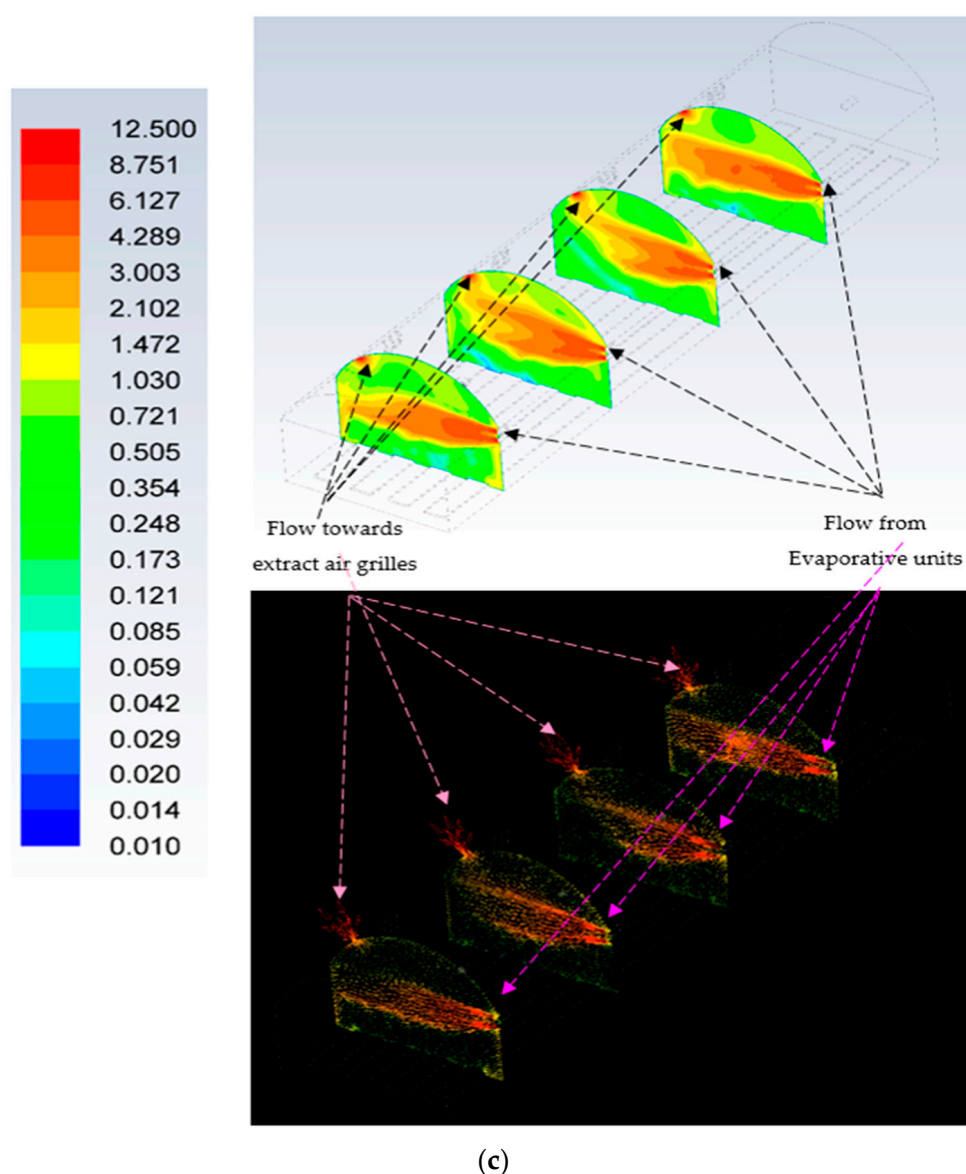
Figure 7. (**a**) Contour plot of air velocity (in m/s) at occupancy level 1, i.e., at a height of z = 1 m from floor level. (**b**) Contour plot of velocity (in m/s) at a height of 1.7 m (XY Plane). (**c**) Contour and vector plots of the air velocity (in m/s) on the XY plane along the length of the greenhouse at various evaporative cooler locations.

5.2. Temperature

Figure 8a,b provides the simulated contour plots of the temperature inside the greenhouse at the occupancy levels of 1 and 2. As with air velocity, the maximum temperature noticed in these simulations exceeded the design criteria. This suggests that the drum diffusers and circulation fans need to be used during the pilot run to bring down those temperatures within desired ranges. The area weighted average temperatures of 21.02 °C and 20.60 °C were obtained at occupancy levels 1 and 2, respectively. As the height from the floor level increased, the area weighted average temperature decreased due to the higher air velocity.

Figure 8c shows the variation of temperature along the length of the greenhouse in the vertical direction near the return air grills placed on the arched portion of the roof. With a high ambient temperature, heat transfer from the ambient to the greenhouse through the polycarbonate sheet is expected to happen. Therefore, the regions near the roof should have a higher temperature than the floor levels. It is seen in Figure 8c that the roof temperature

was around 30 °C, while the floor temperature was mostly 18 °C. As the air at the top was lighter, the air grills could take this air out of the greenhouse and thus set up a flow from the bottom to the top of the greenhouse. Similar results were published by Benni et al., 2016 [22]. The temperature of the floor (height = 0 m) was higher than 21 °C only at a few locations in a sporadic manner. This issue could be addressed during the pilot run by programming the CMS to trigger all of the four circulation fans. It is to be noted in our CFD simulation that only two circulation fans were assumed to be running at full capacity.

Figure 8d shows the temperature profile at different sections transverse to the length of the greenhouse. These sections were chosen to coincide with the location of the evaporative coolers on the right-hand side wall. A higher than desired temperature was observed at certain locations, mostly near the roof, suggesting that this was likely due to the incoming solar radiation. Several regions could also be spotted where the temperature was lower than the desired range. This was due to the air flow from the drum diffusers of the evaporative coolers. Therefore, during the experimental pilot run, the lower drum diffuser angle should be lowered, as that would reduce the minimum temperature observed. Circulation fans should be kept on as well to minimize the high temperature by taking out the hot air by these fans. He et al., 2008 [23], observed similar constraints in their experiments related to greenhouses, and suggested the implementation of a covering material using water films. However, this is not an option under Middle Eastern conditions and therefore was not pursued.

5.3. Relative Humidity

Relative humidity profiles at occupancy levels 1 and 2 are shown as contour plots in Figure 9a,b. Broadly speaking, there are significant portions in these figures where the relative humidity is between 55% to 85%, and is similar to the values obtained in the studies conducted by Villagran et al., 2019 [17] and Kim et al., 2008 [24]. The area weighted average values of the relative humidity were 76.8% and 78.7% at 1 m and at 1.7 m height, respectively. Both of these numbers are well below the upper limit for the crop chosen.

(**a**)
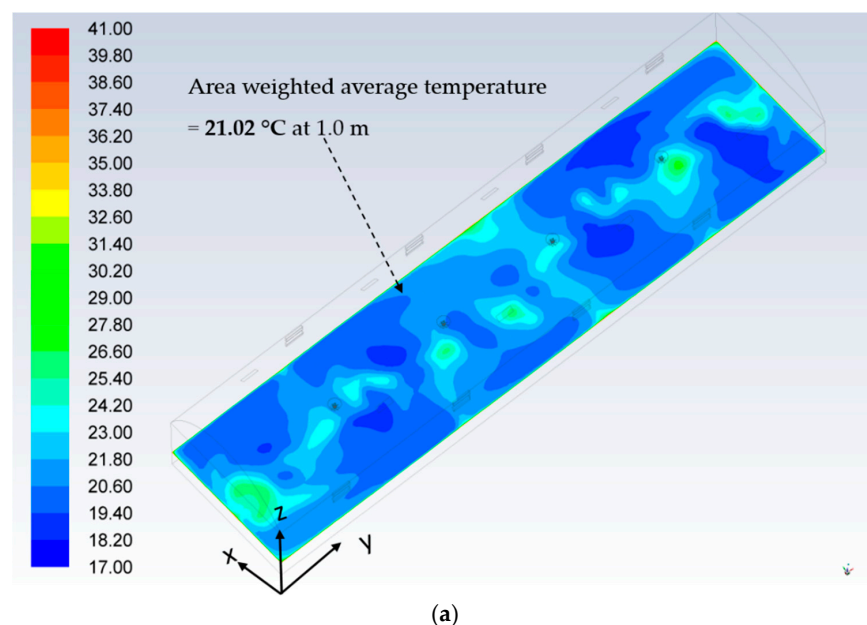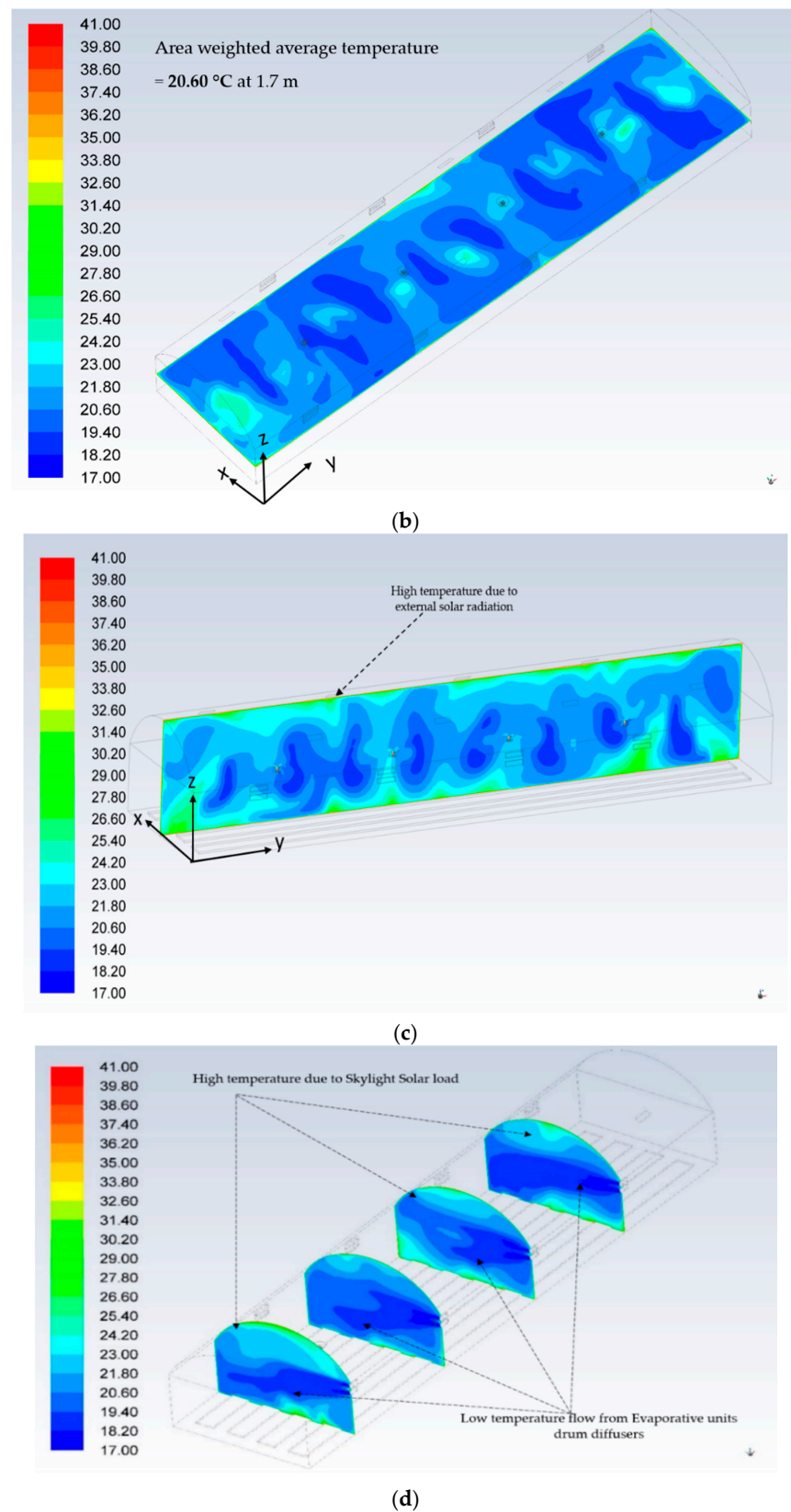
Figure 8. *Cont.*

Figure 8. (**a**) Contour plot of temperature (°C) at a height of 1 m (XY plane). (**b**) Contour plot of temperature (°C) at a height of 1.7 m (XY plane). (**c**) Contour plot of temperature (°C) on (YZ plane) along the length. (**d**) Contour plot of temperature (in °C) along XY plane along length of greenhouse at different evaporative cooler locations.

Figure 9. *Cont.*

(d)
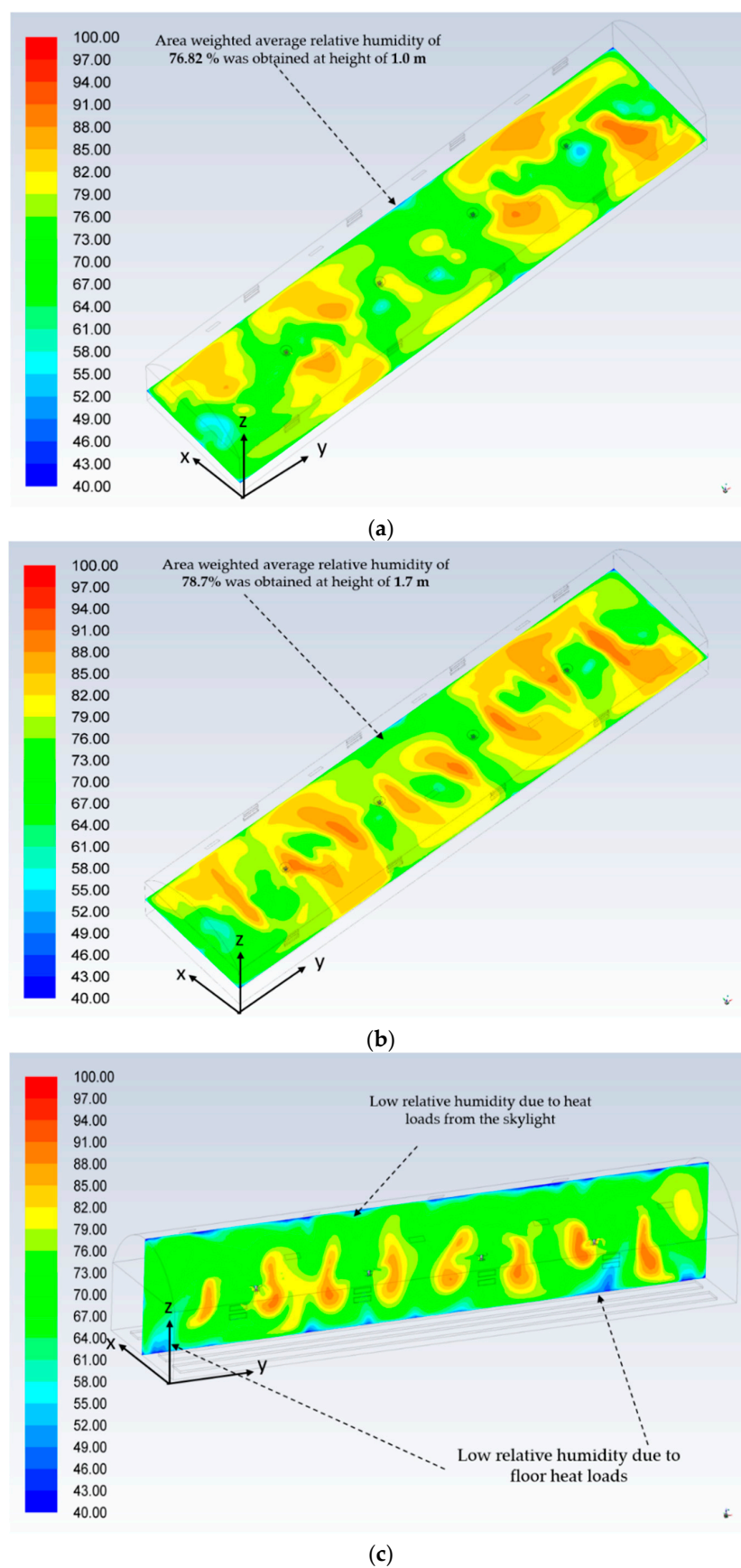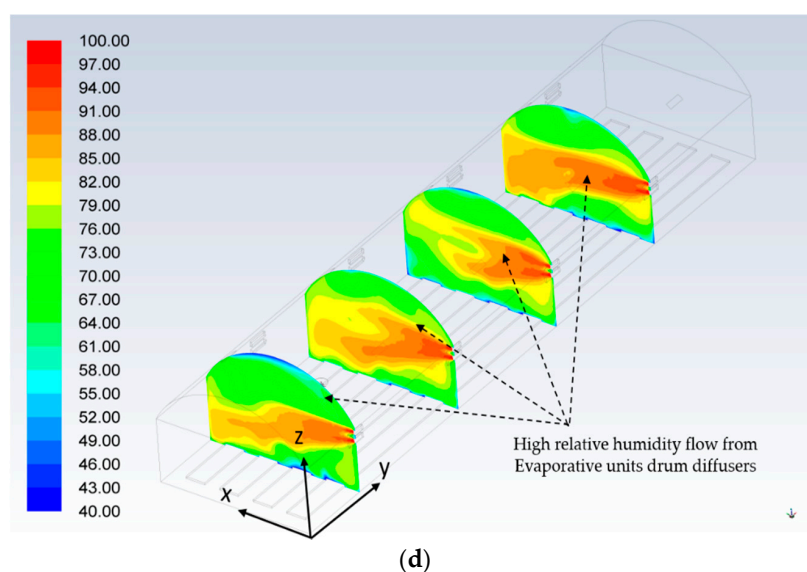
Figure 9. (**a**) Contour plot of relative humidity at a height of 1 m (XY plane). (**b**) Contour plot of relative humidity at a height of 1.7 m (XY plane). (**c**) Contour plot of relative humidity on (YZ plane) along the length. (**d**) Contour plot of relative humidity along XY plane along length of green house at different evaporative cooler locations on one side wall.

As noticed in the air velocity and temperature profiles, it can be seen that at both of these occupancy levels, there were regions where the relative humidity exceeded the desired limits. Again, this was due to the position of the drum diffusers in the box type coolers. The air flowing into the computational domain was relatively more humid than the range required. Therefore, it is not unusual to see more such areas at occupancy level 2 than at 1, as the heights at which the box diffusers were placed was closer to level 2.

Figure 9c represents the variation of relative humidity along the entire length of the greenhouse at a certain locations in the greenhouse. The plane chosen for representing is consistent with the plane chosen previously for presenting the temperature in the previous section. The air grills were also present close to this plane. It is evident that extremely low humidity (~43% to 52%) is seen towards the top left corner and right corners of the plane, and is marked in the figure. As the temperature in those regions is high, the relative humidity can be expected to be lower. Although this is outside the desired range for relative humidity, this is not much of a practical issue as there would be no crops that reach that height, and therefore, this was overlooked during the pilot run.

Figure 9d presents the relative humidity profile along the drum diffusers placed on the right-hand side wall. This is extremely important as the air coming in from the diffuser had 97% relative humidity (refer to Tables 3 and 4 for boundary conditions). The relative humidity around the drum diffuser and in the vicinity was higher than the targeted range of 55–85%. Therefore, the downward tilt on the lower drum diffusers must avoid excessive humidity at or below the crop height level of 1.7 m. The results of the CFD simulation for the air velocity, temperature, and relative humidity at the crop level of 1 m and 1.7 m are summarized below in Table 5.

Table 5. Summary of area weighted average crop growth parameter values from CFD simulations.

Description	Height (m)	Velocity (m/s)	Temperature (°C)	RH (%)
Crop Occupied level	1.0 m	0.435	21.02	76.82
	1.7 m	0.743	20.60	78.70

Some careful generalizations could be made based on the CFD results. Higher temperatures were observed mainly in the regions with the highest airflow, and this was consistent

with what has been reported by Teitel et al., 2008 [25]. In our study, high temperature, higher air velocity, and higher humidity were all correlated either with the solar load or the drum diffuser setting. Studies by Villagran et al., 2018 [26] showed an indoor relative humidity of about 78%. They mentioned that this was mostly due to the high relative humidity of the outdoor air, and could be fixed by optimizing between natural (by air grills) and forced ventilation (by circulation fans). Therefore, for our pilot study, it was necessary to adjust the downward angle of the drum diffusers. In addition, the air grills and circulation fans should be operated based on the feedback received from the CMS in order to achieve the targeted range of crop growth parameters. Elsewhere in commercial greenhouses, mobile dehumidifiers are used to keep RH in control, and we would use these should the pilot run suggest RH hovering outside the target range.

6. Experimental Verification

A pilot run was conducted over a 20-h period on a commercial greenhouse whose details are shared earlier in the experimental setup section. The experimental data measured during the pilot run are discrete, meaning that such data are acquired from spatially localized positions along the tracks mentioned in Figure 3. Therefore, a more suitable metric for comparison of the simulation and experimentally recorded data are the area-weighted average values reported in the Results section before. Additionally, based on the CFD predictions, we needed to make alterations to some of the equipment settings. For example, the angle on the lower drum diffusers at the opening of the air grills could be arranged to be controlled dynamically by the climate management system (CMS). Circulation fans should also be programmed to be turned on in order to avoid higher temperature, air velocity, and relative humidity outside the targeted ranges for the environmental variables. It must be remembered that CFD predictions are for steady state operations, whereas in the pilot study, such steady states may never be achieved due to the continuous change in outdoor parameters (like solar radiation, outdoor temperature, wind velocity, and direction) throughout the day.

The lower drum diffusers for each of the box evaporative coolers were set to 12°. This was necessary as the CFD simulation indicated an air velocity of about 2.1 m/s (Figure 7b) for the BTECs placed closer to the end walls (two BTECs both on the front and rear end). In addition to that, the temperature across the width of the greenhouse was also below 18 °C over a significant portion of the cross section from floor level (Figure 8d). The angle was controlled by a damper at the inlet section. External controls on the damper allowed for a maximum tilt of 18°. As our CFD results were conducted for an angle of 15°, we reduced the angle by 20% of the maximum tilt. The top diffuser angle was kept unchanged. All of the four circulation fans were programmed to be switched on if required (feedback dependent), at a maximum speed equivalent to 5200 CMH. Extra attention was paid to capture the experimental data from locations that showed parameter values outside the permissible range.

For the pilot run using the CMS, set points for crop growth parameters have to be specified on the dashboard of the CMS. Air velocity, temperature, and relative humidity ranges were set as 0.45–0.85 m/s, 18 °C–21 °C, and 13.5–5.5 g/m^3, respectively. Relative humidity between 70–80% was equivalent to 13.5–15.5 g of water vapor per cubic meter of air. This conversion in units had to be done as the RH sensor on the measurement kit directly measures and logs the water vapor content of the air inside the greenhouse.

The variation of experimental data over a 20-h time period is plotted in Figure 10a–c. As the measurement kits could only be moved together, we measured a little over 6 h at heights of 1 m, 1.7 m, and 3.5 m above the greenhouse floor. Among the parameters involved, temperature and RH were considered important only up to the crop height (1.7 m). However, due to the presence of circulation fans, air velocity needed to be considered until a height of 3.5 m. The experimental data shown on the plots at any height are the mean of the data recorded by the measurement kits at that height; also shown on the same plots are the corresponding mean values predicted from CFD simulations at those heights. Readers

should note that the mean value referred here is the arithmetic average of the cells values at that height, i.e., each cell value has equal weightage. This was intentionally done so that we could compare our results to the experimentally measured data, which are not area weighted averages. Fluctuations in experimental values were observed at each of the heights. This was due to the presence of the feedback-based CMS. Whenever the CMS sensed (based on recorded data) that a parameter may exceed the permissible operational range, it generates a feedback signal to mitigate the causes. For example, if it senses high temperature near the roof, if will start the circulation fan for forced ventilation and keep the temperature within the prescribed limits. Likewise, when the temperature goes down, it will stop some of the fans preferentially or close the air grills to prevent the loss of heat.

Figure 10. *Cont.*

(c)
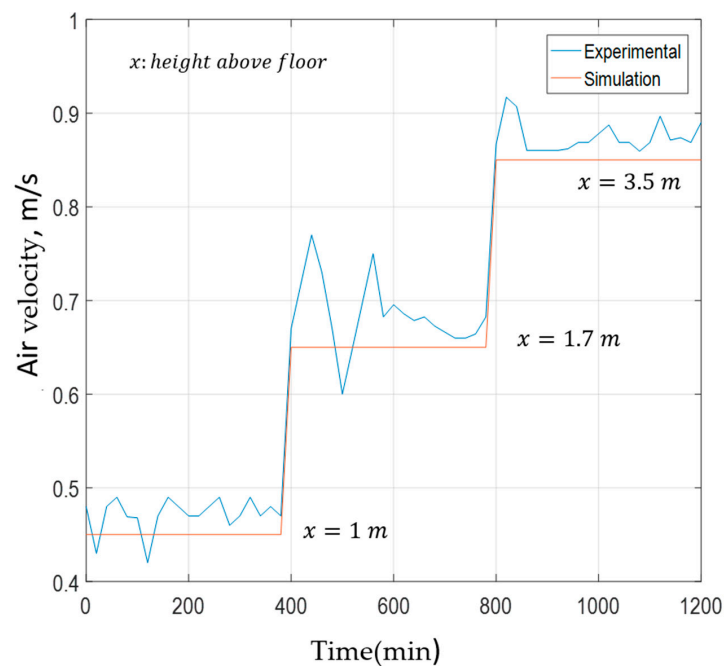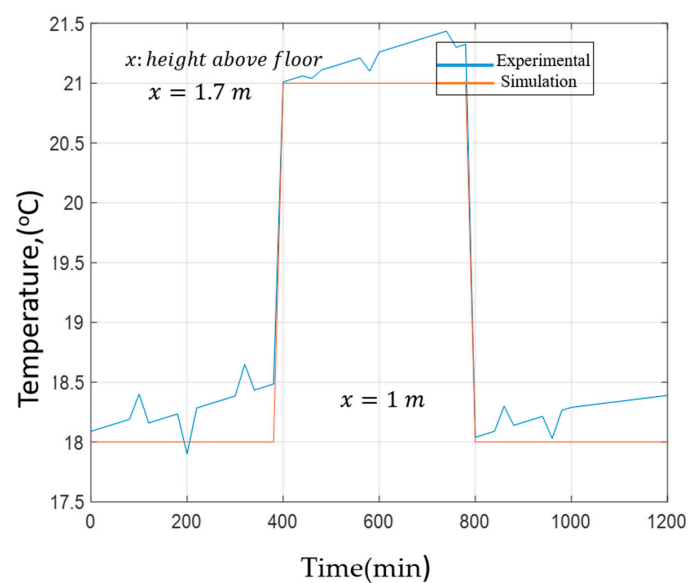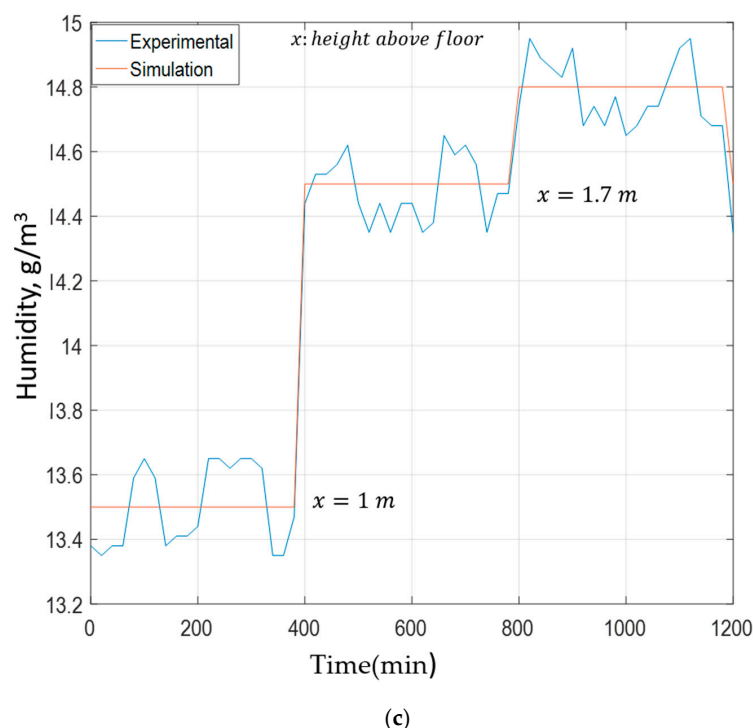
Figure 10. (**a**) Experimental results of air velocity. (**b**) Experimental results for temperature. (**c**) Experimental results for RH.

Plots of the experimentally measured values clearly indicate that the design of the commercial greenhouse is successful in maintaining the crop growth parameters inside the greenhouse. Furthermore, the effectiveness of CFD as a simulation tool in predicting the crop growth parameters in greenhouse agriculture, as mentioned by Li et al., 2019 [27] is also successfully demonstrated. Problems arising due to the buoyancy effect in low external wind speeds (<1.5 m/s), which was simulated by Molina et al., 2011, [28] and Lopez et al., 2011 [29], is avoided in this design. Use of both natural and mechanical ventilation, blended with a climate control interfaced platform, is thus capable of achieving the desired objective. The temperature values obtained in the pilot run were below the threshold of 40 °C recommended by Villagran et al., 2019 [30].

Experimentally recorded data of the crop growth parameters at occupancy level 2, i.e., at a height of 1.7 m from the floor, are shown in Table 6. Placed in adjacent columns are the mean values for the same parameters obtained from the CFD analysis. The standard deviation and the range for these data sets obtained during the experiments and from CFD results are also mentioned in the same table. Standard deviation in the table is a measure of dispersion, signifying the spread of the individual values in the sample data from the arithmetic mean. The range shows the minimum and maximum values in the sample data considered. The experimental data clearly prove that all the crop parameters were well within their desired ranges during the hot summer day chosen for conducting the trial run.

Table 6. Simulated and experimental statistics for air velocity, temperature, and humidity at a height of 1.7 m.

Criteria	Mean		Std. Deviation		Range	
	Simulated	**Experimental**	**Simulated**	**Experimental**	**Simulated**	**Experimental**
Air Velocity	0.65	0.68	0.16	0.17	0.49–0.82	0.5–0.88
Temperature	18.98	19.23	1.41	1.40	17.58–20.39	18.06–20.88
Humidity $* \left(\text{g m}^{-3} \right)$	14.27	14.25	0.55	0.84	13.72–14.8	13.31–15

* RH from CFD results, expressed as %, is converted to "humidity" and calculated as grams of water vapor per unit volume of air (g m^{-3}).

Table 6 shows the arithmetic mean of the environmental variables at a height of 1.7 m above floor level. This was done to make a fair comparison between experimental data obtained from measurement kits and CFD simulation. The text and figures in the results section refer to area weighted values, where the average is calculated by multiplying the local values by a weighing factor. In this case, the weighing factors are the respective areas. This was done in accordance with existing practice, as suggested in the literature. Therefore, these numbers are distinct and should not be confused.

The proximity of the mean values between the experimental and CFD data justifies the use of CFD simulations in the process of the greenhouse design. Modification to the inlet angle of the lower drum diffusers was carried out based on the CFD predictions. Likewise, the circulation fans were also programmed in the CMS to run whenever needed. The importance of the CFD simulation could never be emphasized enough in fine tuning the CMS for the experiments. The pilot run clearly shows that the commercial greenhouse designed using BTECs and interfaced with the CMS module is capable of keeping the crop growth parameters within necessary ranges in Middle East climatic conditions. The feasibility of the use of BTECs as opposed to the conventional fan-cooling pad-based technology is demonstrated on a pilot basis.

7. Conclusions

This study describes the design of a commercial greenhouse in Dubai employing new technology in the form of BTEC coolers in HVAC systems. The greenhouse is also fitted with a completely automated CMS. A full-scale CFD simulation is performed using ANSYS Fluent for typical peak summer conditions to predict the spatial distribution of the crop growth parameters inside the greenhouse in general. Special interest is paid to the values at a crop height level of 1.7 m from the floor. The results of the CFD simulation are interpreted and utilized in carrying out a 20-h pilot run for the greenhouse. The downward angle of the lower drum diffusers is set to 12° for the pilot run to avoid a low temperature near the floor level. Experimentally recorded data suggest that the crop growth parameters are within the crop-specific prescribed range. Average air velocity, temperature, and relative humidity are found to be 0.68 m/s, 19.23 °C and 76.2%, respectively, at a crop height of 1.7 m, which is shown to be close to the average values predicted in our CFD simulation. This paper therefore clearly demonstrates the successful operation of an automated, CMS enabled commercial greenhouse using new BTECs.

Author Contributions: S.M.C. developed the upgraded model for the commercial greenhouse and conducted the experimental evaluation and CFD simulation. S.C. has formulated the structure of the paper and provided valuable inputs towards the CFD simulation. R.K. managed the entire technical paper in terms of technical improvements and quality of the paper. All authors have read and agreed to the published version of the manuscript.

Funding: This research received no external funding.

Acknowledgments: I would sincerely like to thank all the faculties and staff in Department of Mechanical Engineering at BITS Pilani Dubai Campus for their guidance and support that was instrumental in the presentation of this research paper.

Conflicts of Interest: The authors declare no conflict of interest.

Abbreviations

HVAC	Heating Ventilation and Air conditioning
CFD	Computational fluid dynamics
WIS	wireless irrigation system
PAR	Photo-Synthetically Active Radiation.
PI	Proportional-integral
PID	Proportional-integral-derivative
CMH	Cubic minutes per hour.

References

1. Ghani, S.; ElBialy, E.M.A.A.; Bakochristou, F.; Gamaledin, S.M.A.; Rashwan, M.M. The effect of forced convection and PCM on helmets' thermal performance in hot and arid environments. *Appl. Therm. Eng.* **2017**, *111*, 624–637. [CrossRef]
2. Liu, B.; Qu, J.; Niu, Q.; Wang, J.; Zhang, K. Computational fluid dynamics evaluation of the effect of different city designs on the wind environment of a downwind natural heritage site. *J. Arid Land* **2014**, *6*, 69–79. [CrossRef]
3. Lefers, R.; Bettahalli, N.M.S.; Nunes, S.P.; Fedoroff, N.; Davies, P.A.; Leiknes, T.O. Liquid desiccant dehumidification and regeneration process to meet cooling and freshwater needs of desert greenhouses. *Desalin. Water Treat.* **2016**, *57*, 23430–23442. [CrossRef]
4. Taki, M.; Mehdizadeh, S.A.; Rohani, A.; Rahnama, M.; Rahmati-Joneidabad, M. Applied machine learning in greenhouse simulation; new application and analysis. *Inf. Process. Agric.* **2018**, *5*, 253–268. [CrossRef]
5. Dai, Y.; Sumathy, K. Theoretical study on a cross-flow direct evaporative cooler using honeycomb paper as packing material. *Appl. Therm. Eng.* **2002**, *22*, 1417–1430. [CrossRef]
6. ASHRAE. *ASHRAE Handbook—HVAC Applications*; American Society of Heating (ASHRAE): Atlanta, GA, USA, 2011.
7. Mobtaker, H.G.; Ajabshirchi, Y.; Ranjbar, S.F.; Matloobi, M. Solar energy conservation in greenhouse: Thermal analysis and experimental validation. *Renew. Energy* **2016**, *96*, 509–519. [CrossRef]
8. Kuroyanagi, T. Investigating air leakage and wind pressure coefficients of single-span plastic greenhouses using computational fluid dynamics. *Biosyst. Eng.* **2017**, *163*, 1527. [CrossRef]
9. Perret, J.S.; Al-Ismaili, A.M.; Sablani, S.S. Development of a humidification–dehumidification aystem in a quonset greenhouse for sustainable crop production in arid regions. *Biosyst. Eng.* **2005**, *91*, 349–359. [CrossRef]
10. Franco, A.; Valera, D.L.; Peña, A. Energy Efficiency in Greenhouse Evaporative Cooling Techniques: Cooling Boxes versus Cellulose Pads. *Energies* **2014**, *7*, 1427–1447. [CrossRef]
11. Wu, F.; Xu, F.; Zhang, L.; Ma, X. Numerical simulation on thermal environment of heated glass greenhouse based on porous medium. *Trans. Chin. Soc. Agric. Mach.* **2011**, *42*, 180–185.
12. Boulard, T.; Roy, J.C.; Pouillard, J.B.; Fatnassi, H.; Grisey, A. Modelling of micrometeorology, canopy transpiration and photosynthesis in a closed greenhouse using computational fluid dynamics. *Biosyst. Eng.* **2017**, *158*, 110–133. [CrossRef]
13. Chu, C.R.; Lan, T.W.; Tasi, R.K.; Wu, T.R.; Yang, C.K. Wind-driven natural ventilation of greenhouses with vegetation. *Biosyst. Eng.* **2017**, *164*, 221–234. [CrossRef]
14. Ghani, S.; Bakochristou, F.; ElBialy, E.M.A.A.; Gamaledin, S.M.A.; Rashwan, M.M.; Abdelhalim, A.M.; Ismail, S.M. Design challenges of agricultural greenhouses in hot and arid environments—A review. *Eng. Agric. Environ. Food* **2019**, *12*, 48–70. [CrossRef]
15. Guo, J.; Liu, Y.; Lü, E. Numerical Simulation of Temperature Decrease in Greenhouses with Summer Water-Sprin kling Roof. *Energies* **2019**, *12*, 2435. [CrossRef]
16. Launder, B.E.; Spalding, D.B. The Numerical Computation of Turbulent Flows. *Comput. Methods Appl. Mech. Eng.* **1974**, *3*, 269–289. [CrossRef]
17. ANSYS. Available online: https://www.ansys.com/ (accessed on 3 July 2021).
18. Villagrán Munar, E.A.; Bojacá Aldana, C.R. Simulación del microclima en un invernadero usado para laproducción de rosas bajo condiciones de clima intertropical. *Chil. J. Agric. Anim. Sci.* **2019**, *35*, 137–150.
19. Moureh, J.; Menia, N.; Flick, D. Numerical and experimental study of airflow in a typical refrigerated truckconfiguration loaded with pallets. *Comput. Electron. Agric.* **2002**, *34*, 25–42. [CrossRef]
20. Baeza, E.J.; Pérez-Parra, J.J.; Lopez, J.C.; Montero, J.I. CFD study of the natural ventilation performance of aparral type greenhouse with di_erent numbers of spans and roof vent configurations. *Acta Hortic.* **2006**, *719*, 333–340. [CrossRef]
21. Katsoulas, N.; Bartzanas, T.; Boulard, T.; Mermier, M.; Kittas, C. Effect of Vent Openings and Insect Screenson Greenhouse Ventilation. *Biosyst. Eng.* **2006**, *93*, 427–436. [CrossRef]
22. Benni, S.; Tassinari, P.; Bonora, F.; Barbaresi, A.; Torreggiani, D. Efficacy of greenhouse natural ventilation: Environmental monitoring and CFD simulations of a study case. *Energy Build.* **2016**, *125*, 276–286. [CrossRef]
23. He, J.; Hoyano, A. A numerical simulation method for analyzing the thermal improvement effect of super-hydrophilic photocatalyst-coated building surfaces with water film on the urban/built environment. *Energy Build.* **2008**, *40*, 968–978. [CrossRef]
24. Kim, K.; Yoon, J.-Y.; Kwon, H.-J.; Han, J.-H.; Son, J.E.; Nam, S.-W.; Giacomelli, G.A.; Lee, I.-B. 3-D CFD analysis of relative humidity distribution in greenhouse with a fog cooling system and refrigerative dehumidifiers. *Biosyst. Eng.* **2008**, *100*, 245–255. [CrossRef]
25. Teitel, M.; Liran, O.; Tanny, J.; Barak, M. Wind driven ventilation of a mono-span greenhouse with a rose crop and continuous screened side vents and its effect on flow patterns and microclimate. *Biosyst. Eng.* **2008**, *101*, 111–122. [CrossRef]
26. Villagran Munar, E.A.; Bojacá Aldana, C.R.; Rojas Bahamon, N.A. Determinación del comportamientotérmico de un invernadero espacial colombiano mediante dinámica de fluidos computacional. *Rev. UDCA Actual. Divulg. Científica* **2018**, *21*, 415–426.
27. Li, K.; Xue, W.; Mao, H.; Chen, X.; Jiang, H.; Tan, G. Optimizing the 3D Distributed Climate inside Greenhouses Using Multi-Objective Optimization Algorithms and Computer Fluid Dynamics. *Energies* **2019**, *12*, 2873. [CrossRef]
28. Molina-Aiz, F.D.; Valera, D.L.; López, A. Airflow at the openings of a naturally ventilated Almería-type greenhouse with insect-proof screens. *Acta Hortic.* **2011**, *893*, 545–552. [CrossRef]

29. López, A.; Valera, D.L.; Molina-Aiz, F. Sonic anemometry to measure natural ventilation in greenhouses. *Sensors* **2011**, *11*, 9820–9838. [CrossRef] [PubMed]
30. Villagrán, E.A.; Bojacá, C.R. Study of natural ventilation in a Gothic multi-tunnel greenhouse designed toproduce rose (*Rosa* spp.) in the high-Andean tropic. *Ornam. Hortic.* **2019**, *25*, 133–143.